ACS APPLIED MATERIALS & INTERFACES

Research Article

www.acsami.org

Adhesive and Reinforcing Properties of Soluble Cellulose: A Repulpable Adhesive for Wet and Dry Cellulosic Substrates

Elisa S. Ferreira,[†,‡] Evandro M. Lanzoni,[†] Carlos A. R. Costa,[†] Christoph Deneke,[†] Juliana S. Bernardes,[†] and Fernando Galembeck*[,†,‡]

[†]National Nanotechnology Laboratory (LNNano), National Center for Energy and Materials (CNPEM), Campinas, São Paulo, Brazil 13083-970

[‡]Institute of Chemistry, University of Campinas - UNICAMP, P.O. Box 6154, Campinas, São Paulo, Brazil 13083-970

Supporting Information

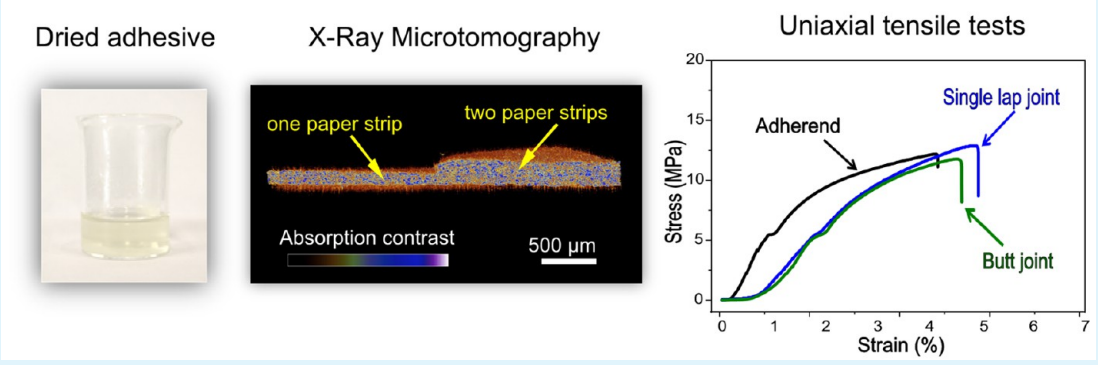

ABSTRACT: This work reports, for the first time, the excellent performance of an aqueous alkaline solution of cellulose as an adhesive for wet and dry cellulosic substrates. Uniaxial tensile tests of filter paper and sulfite writing paper strips bonded with this adhesive (5% cellulose and 7% NaOH aqueous solution) show that failure never occurs in the joints but always in the pristine substrate areas, except in butt joint samples prepared with sulfite paper. Tensile test also shows that paper impregnated with cellulose solution is stronger than the original substrate. X-ray microtomography and scanning electron microscopy reveal that dissolved cellulose fills the gaps between paper fibers, providing a morphological evidence for the mechanical interlocking adhesion mechanism, while scanning probe techniques provide a sharp view of different domains in the joints. Additionally, bonded paper is easily reconverted to pulp, which facilitates paper reprocessability, solving a well-known industrial problem related to deposition of adhesive aggregates (stickies) on the production equipment.

KEYWORDS: *adhesive, cellulose, repulpable, wet substrates, alkaline dissolution*

1. INTRODUCTION

Cellulose is the most abundant natural biopolymer on earth, with an annual global production of 1×10^{11} to 1×10^{12} tons,[1] widely used in textiles as cotton, flax, and regenerated cellulose fiber, or in paper and board. It is also a versatile reagent for chemical conversion, yielding important thermoplastics and polyelectrolytes. In many applications, dissolving cellulose is a crucial fabrication step. However, cellulose does not dissolve in water or in any common solvents, and early industrial processes used complex solvents whose utilization is currently restricted because of environmental and economic issues.[1,2]

Many researchers targeted the development of new "greener" and nondegrading cellulose solvents during the last few decades, including ionic liquids.[3] The only solvent used on large scale today is *N*-methylmorpholine N-oxide (NNMO) hydrate,[4] which produces regenerated cellulose fibers with high crystallinity. Another promising green solvent was developed by Kamide et al. in 1987,[5] when steam-exploded chemical pulp from wood was dissolved in aqueous NaOH solution at low temperature (−5 °C), without the addition of any other reagent. Later, Attala et al.[6] showed that many cellulose samples with different molecular weights, degrees of crystallinity and obtained from different sources can also be dissolved using this procedure. A detailed DSC work by the Navard group revealed that the limit for cellulose dissolution in NaOH/water is at least four NaOH molecules per one anhydroglucose unit or else, the weight ratio of cellulose to NaOH is close to unity.[7]

These findings triggered intensive study aiming the production of polymer materials from alkaline cellulose solutions, often using urea as a cosolubilizing agent. Zhang et al. prepared films,[8] membranes,[9] fibers,[10,11] and nanocomposites,[12] while regenerated nanocellulose particles from NaOH solution were obtained by Bansal et al.,[13] opening a broad range

Received: June 15, 2015
Accepted: August 4, 2015
Published: August 4, 2015

DOI: 10.1021/acsami.5b05310
ACS Appl. Mater. Interfaces 2015, 7, 18750−18758

of technological applications, including nanocomposites, biofuels and drug delivery systems.

Solutions from, for example, polystyrene, acrylics, and polyene rubbers, are effective adhesives for the respective polymer solids but this approach is often ineffective using semicrystalline or cross-linked polymers due to limited entanglement of adhesive and substrate chains.[14] Surprisingly, the adhesive properties of cellulose alkaline solutions have not yet been determined and many researchers agree with Baumann and Conner stating that cellulose cannot be used in the formulation of adhesives, due its insolubility in common solvents. However, there are adhesives made using cellulose ether and ester solutions for several applications, when inexpensive means to bond porous solids are required. Cellulosic thermoplastics have also been used as hot-melt adhesives.[14]

Bonding paper and other cellulosic materials is usually a simple task, since these are high surface-energy porous solids, easily wetted by almost any adhesive solution or dispersion. However, bonding paper with other polymers creates a problem for paper recycling, since the adhesive residues aggregate forming masses of extraneous materials (stickies) in the repulping process, contaminating the recycled product and eventually causing equipment malfunctioning.[15] Some available alternatives are hot-melt adhesives[16] and water-dispersible polymers, such as acrylic monomers with modified polyethylene terephthalate,[17] which are petrochemical products.

An additional requirement for some applications is the ability of the adhesive to bond wet paper. Pelton et al. developed several adhesives based on proteins[18,19] and on PVAm[20−22] for wet regenerated cellulose, forming covalent bonds to achieve adhesion. In these works, 2,2,6,6-tetramethyl-1-piperidinyoxy (TEMPO) mediated oxidation of cellulose surface is used to enhance the wet tensile strength.

In this paper, we employed a simple cellulose alkaline solution, containing only NaOH, cellulose, and water, as adhesive and reinforcing agent for dry and wet paper. Our results reveal the good mechanical performance of wet and dry adhesive joints prepared with two different cellulosic adherends (filter paper and sulfite paper). The paper joints form pulp by mechanical redispersion, undistinguishable from the as-received paper sheets, thus allowing paper reprocessability.

2. EXPERIMENTAL SECTION

Materials. Cotton linter cellulose (high purity grade) and NaOH (≥98% purity) used to prepare cellulose solutions were from Sigma-Aldrich. NaCl (≥99.5% purity) from Merck was used to prepare aqueous NaCl solution for wet adhesion measurements. Qualitative filter paper (80 g/m^2) from Unifil and sulfite paper (75 g/m^2) from Suzano were used as adherends. PVAc white glue from BIC was used for the sake of comparison.

Cellulose Adhesive Solution. Cellulose powder (5% w/w) was added to NaOH (7% w/w) aqueous solution at 0 °C and stirred for 10 min at 6000 rpm using an Ultra Turrax apparatus (IKA). The mixture was then cooled down to −20 °C for 1 h, defrosted at room temperature, shaken, and used as adhesive solution.

Assembly of Adhesive Joints. (a) Single lap joints: 40 mg of cellulose solution was spread over 2.5 cm^2 of dry or wet (60% w/w water) filter paper strips (100 mm × 25 mm × 0.12 mm) and sulfite paper strips (100 mm × 25 mm × 0.09 mm). Specimen and adhesive joint dimensions were adopted from ref 23. Each strip was joined to a similar one under ca. 700 mN compression force, applied during 5 s. (b) Butt joint: torn edges of two paper strips were immersed 2 mm into the cellulose adhesive solution and their wetted edges were joined. Lap and butt joints were let to dry at 24 °C for 180 min. (c) Impregnated strip: filter paper strips (175 mm × 25 mm × 0.12 mm) were completely immersed in the cellulose solution during 60 s and then suspended by tweezers for 20 s. The solution excess was removed by compression force of ca. 700 mN, applied during 5 s, between two filter paper strips (200 mm × 30 mm × 0.12 mm). Finally, the impregnated strip dried at room temperature during 24 h and the paper thickness rises from 0.12 to 0.19 mm after coating. Figure 1 shows the geometry of samples prepared using paper strips.

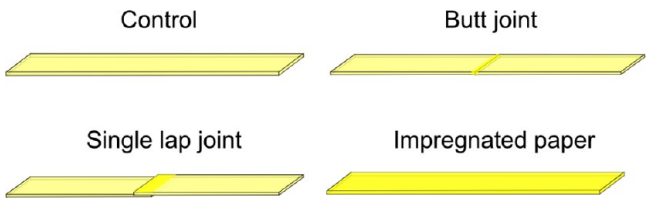

Figure 1. Graphic representation of the paper strip, glued, and impregnated specimens prepared; adhesive-coated areas are represented in yellow.

Repulping Test. Five glued samples prepared using filter paper and cellulose solution (5% cellulose and 7% NaOH) were wet-milled in a blender (Walita) during 10 min, then the mixture was allowed to settle for 30 min. The same procedure was used on paper strips glued with a commercial PVAc emulsion, used as a control.

Mechanical Characterization. An Emic DL2000 equipment was used to perform the uniaxial tensile tests. Prior to the characterization, 10 samples of each substrate-adhesive system were conditioned at 23 ± 2 °C and 50 ± 5% humidity for 40 h. For wet adhesion evaluation, single lap joint samples were immersed in NaCl 1 mM solution for 30 min at pH 6.[24] Excess water was removed by compression (ca. 700 mN) between two filter paper strips (200 mm × 30 mm × 0.12 mm) during 5 s, and then the uniaxial tensile test was immediately carried out. The specimen working length used for adhesive joints and impregnated samples was 140 mm and the constant speed adopted was 1.25 mm/min,[23] until failure. Data treatment considered Gaussian distribution for all samples.

Scanning Electron Microscopy (SEM). Scanning electron micrographs of the samples were obtained on a SEM-FEG *FEI* Quanta 650 microscope operating at 5 kV accelerating voltage and spot size 5.5. Samples were fixed with copper tape on a stub and sputtered with gold (16 nm) using a Bal-Tec SCD 005 Coater.

Microtomography. Filter paper, adhesive joint, and impregnated strips were scanned using a Skyscan −1272 (Bruker) instrument operating at 20 kV, 145 μA, 0.2° step rotation, 4 frames per position and 2.5 μm nominal resolution (2452 × 1640). NRecon software (v. 1.6.9.8, SkyScan) was used to reconstruct cross-section images from microtomography projections to 3D images, using Feldkamp algorithm. For reconstruction, ring artifact and beam hardening correction parameters were fixed at zero and smoothing correction level one was applied to reduce the noise. The same X-rays attenuation contrast limits were selected for all samples, allowing comparisons. CTVOx software (v. 2.2.3.0, SkyScan) was used for 3D visualization and image acquisition. Specific surface roughness values were calculated for a random volume of interest (VOI) in each sample measuring 0.04 mm × 0.8 mm and divided in 300 slices, using CTan software (v. 1.14.4.1, SkyScan).

Atomic Force Microscopy (AFM). Topography, phase contrast, electric potential, and capacitance gradient (dC/dz) images of the adhesive-substrate systems were obtained in a NX-10 Atomic Force Microscope (Park System) in intermittent contact mode. A NCHR probe (NanoWorld) with a spring constant of 42 N m^{-1}and 320 kHz resonance frequency was used for phase contrast measurements and an EFM probe (NanoWorld) with spring constant of 2.8 N m^{-1} and resonance frequency within 75 kHz was used for electrical measurements. Prior to AFM imaging, the cellulose samples were fixed on metal samples stubs using a double-sided adhesive tape.

DOI: 10.1021/acsami.5b05310
ACS Appl. Mater. Interfaces 2015, 7, 18750−18758

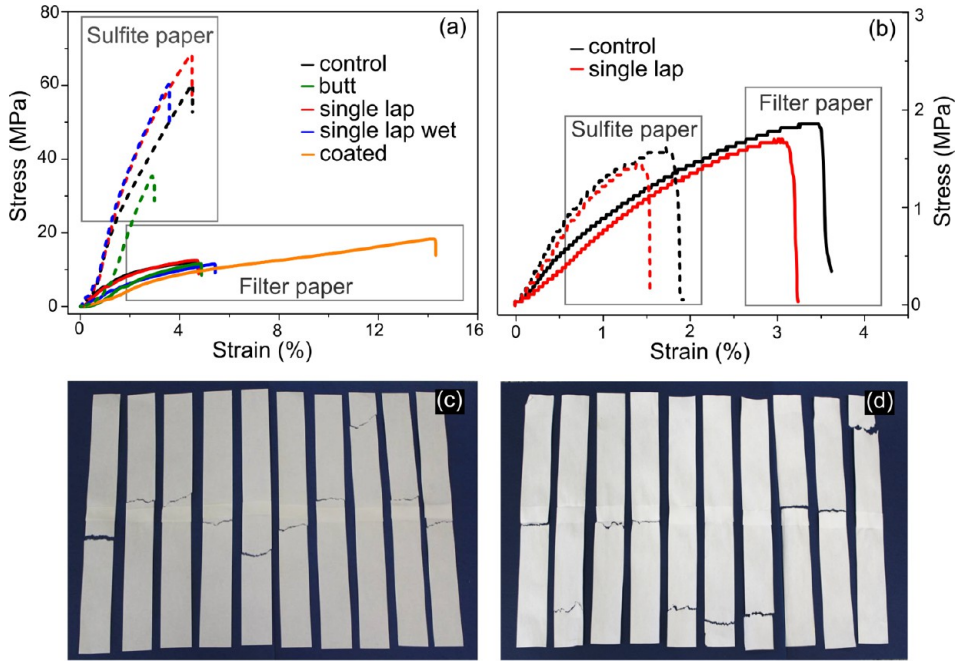

Figure 2. Stress–strain diagrams: (a) dry filter (FP) and sulfite paper (SP) strips bonded with cellulose adhesive; (b) wet-tested FP and wet-tested SP strips bonded with cellulose adhesive. Pictures from tested samples: (c) dry-tested FP lap joint samples and (d) wet-tested SP lap joint samples.

Electric potential and capacitance coupling measurements followed procedures described in the literature,[25,26] applying a second AC signal at 17 kHz to the metal-coated cantilever. The electric potential of the sample is measured by applying a DC potential to the cantilever and bringing down its response to zero, in this AC frequency. Furthermore, we monitor the second harmonic of the AC signal, which is shown to be proportional to the capacitance gradient (dC/dz) or capacitance coupling of the tip to the sample.[27] Following the literature,[27] we know that the signal in the second harmonic is proportional to $(C_{eff}/C_{air})^2\, dC_{air}/dz$, with C_{eff} as the total capacity of the sample and tip, C_{air} the capacity of the tip-air gap and z the sample distance. The effective capacitance of the system is the reciprocal of the sum of the reciprocal component capacitances: $1/C_{eff} = 1/C_{air} + \Sigma 1/C_{sample}$, where $\Sigma 1/C_{sample}$ is the sum of the sample contributions from the filter paper and the adhesive film.

3. RESULTS AND DISCUSSION

To investigate the mechanical quality of the adhesive joints, we carried out uniaxial tensile tests on three different types of filter paper (FP) joints (a single lap joint, a wet bonded single lap joint and a butt joint) as well as on FP impregnated with the adhesive and on control strips of the pristine filter paper. Plots of the strain as a function of stress applied to the samples are presented as solid lines in Figure 2a and also in Table S1. In Figure 2a, we show one individual curve for each sample type (joined paper, impregnated paper and control). The behavior of the glued paper strips is very close to the pristine paper strip: they undergo an initial small elastic deformation followed by a larger plastic deformation, until it breaks under ca. 12 MPa, closely the same for all samples. On the other hand, filter paper strips impregnated with the cellulose solution are more resistant to tension than the control: the maximum tensile stress rises to 18 MPa and the maximum elongation is almost 15%, 3 times higher than the untreated paper sheets.

Similar experiments were made using sulfite paper (SP) and the results are also in Figure 2a. In general, all SP samples reach a higher stress at the same strain than the FP samples, due to their higher elastic modulus. SP samples bonded by single lap joints show a maximum stress close to 60 MPa (blue and red dashed lines in Figure 2a, comparable to the control (black, dashed line) and ca. 5 times the value of the FP.

Together, these results show that the adhesive joints are stronger than the respective paper adherends, except in the case of butt joints made with sulfite paper strips.

We also tested wet FP and SP single lap joints and the corresponding strain–stress curves are shown in Figure 2b. The maximum stress reached for FP and SP single lap joints was 1.7 and 1.4 MPa, respectively. Again, failure never took place at the adhesive joint.

Pictures of dry and wet tested samples are shown Figure 2c, d, showing rupture outside of the bonded area.

Our uniaxial tensile tests demonstrate that alkaline cellulose solutions are effective adhesives for wet and dry paper and the bonded areas resist mechanical tension, better than the substrates themselves, with one only exception: dry butt joints assembled with sulfite paper.

To understand the excellent mechanical properties of our cellulose-based adhesive, a detailed investigation of the microstructure of the joints followed. Figure 3 shows SEM images of filter paper substrate and of bonded areas. Comparing the images of the joints with the as-received FP, we see the adhesive filling the pores between the fibers (Figures 3b–f); this is not only observed in the top view images (Figure 3b, d–f) but also in the cross-section micrograph in Figure 3c. The adhesive solution permeates the wet substrates even better than the dry ones, as observed in Figure 3d were the filling material is more evenly distributed across the paper surface. Finally, the SEM image of the butt joint in Figure 3e shows two joined pieces of paper embedded in a continuous cellulose matrix. Unlike the joints seen in Figure 3b, d, the interface between the two stripes is only faintly visible, indicating the good adjunction of the two pieces. The good penetration and distribution of the adhesive also contributes to the observed increase of impregnated FP stretching ability verified during uniaxial tensile test. As the adhesive not only coats but also penetrates

DOI: 10.1021/acsami.5b05310
ACS Appl. Mater. Interfaces 2015, 7, 18750–18758

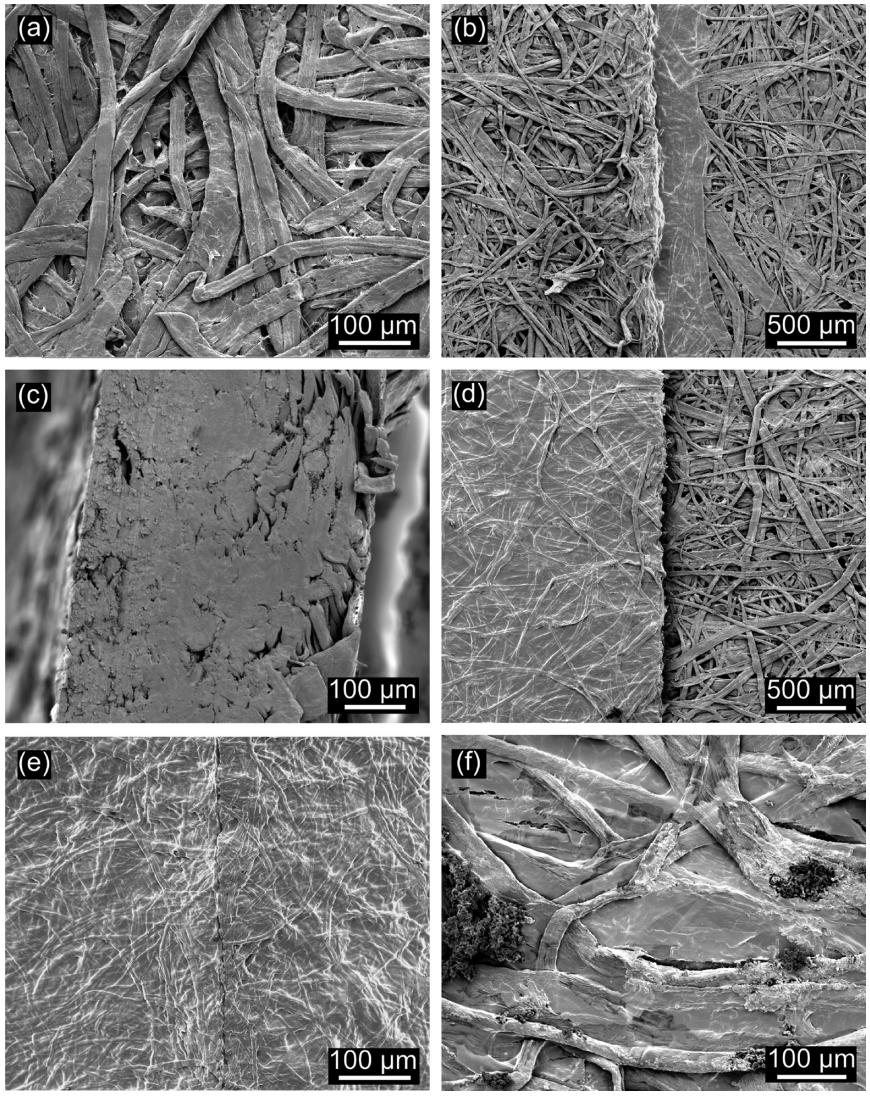

Figure 3. Secondary electron images of: (a) as-received filter paper surface; (b) filter paper strips bonded with cellulose adhesive, single lap joint surface; (c) cross-section view of b; (d) single lap joint prepared with wet strips; (e) butt joint; (f) impregnated single strip.

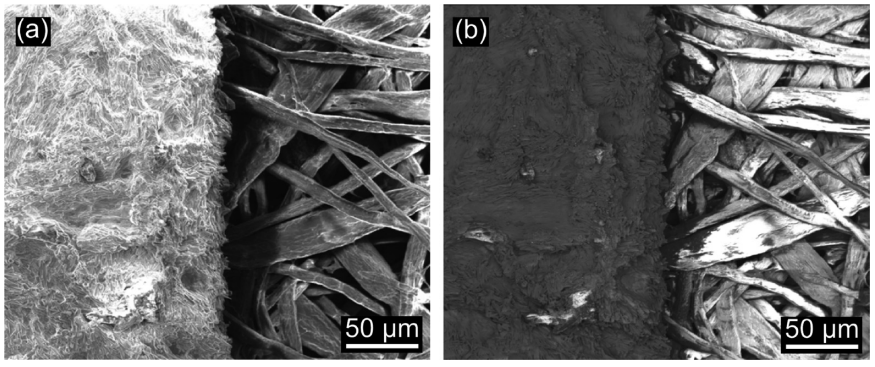

Figure 4. Single lap joint prepared with wet filter paper strips and cellulose adhesive, imaged using (a) secondary electrons and (b) backscattered electrons.

the paper pores, the result is a kind of new composite material with a higher plasticity than filter paper, analogous to other fiber/polymer compounds.

Figure 4 shows micrographs of the same area from a lap joint but using secondary and backscattered electrons, where contrast in the latter is determined by the average atom number in each pixel. In both images, the strip with adhesive is to the left, whereas extant paper adjacent to the joint is to the right, for the sake of comparison. The left side of the backscattered electrons image is uniformly dull, as expected due to the low crystallinity of the adhesive cellulose and it shows that it penetrates the paper voids. The few bright spots in the

DOI: 10.1021/acsami.5b05310
ACS Appl. Mater. Interfaces 2015, 7, 18750−18758

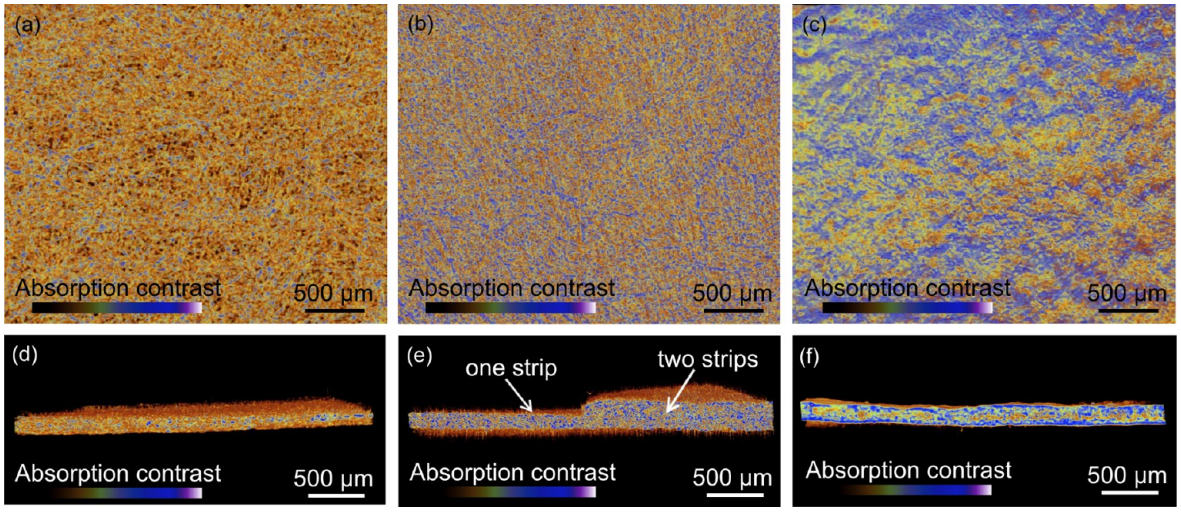

Figure 5. Reconstructed images from X-ray microtomography: top and cross section views of (a, d) as-received filter paper strip, (b, e) single lap joint prepared with wet strips and (c, f) impregnated filter paper.

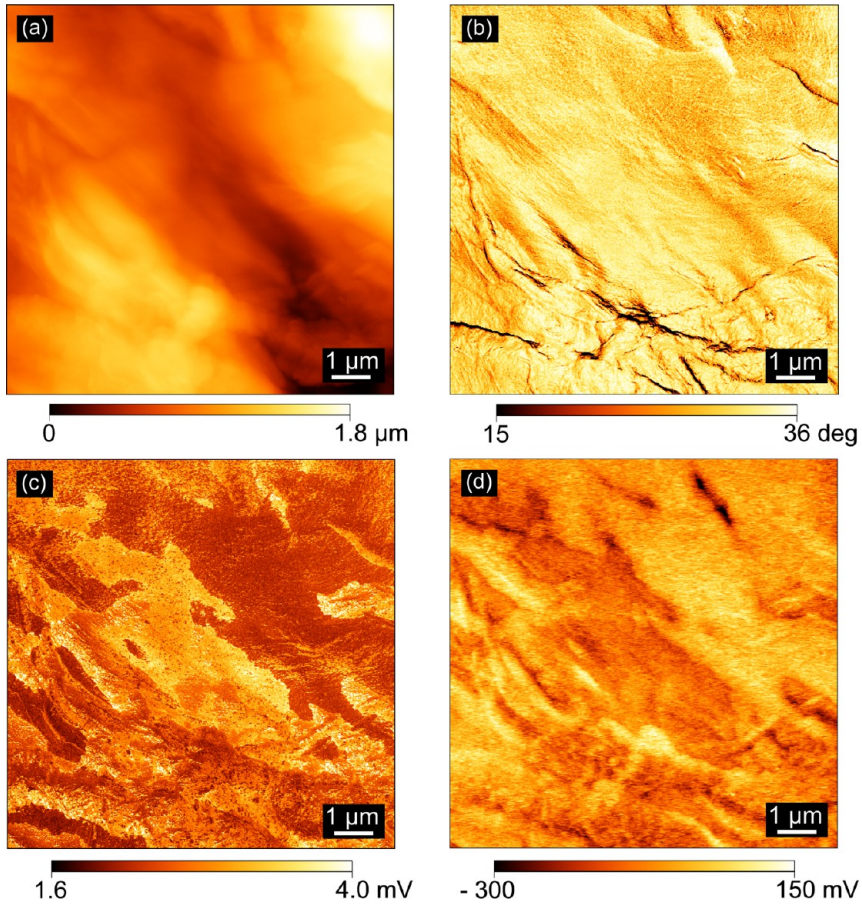

Figure 6. Micrographs from cellulose adhesive dried on filter paper: (a) topography, (b) phase-contrast, (c) dC/dz, and (d) electric potential maps.

middle of adhesive cellulose are expected, because of the presence of residual sodium carbonate crystals.

The main difficulty in using this adhesive is the use of alkali that restricts it to industrial or laboratory environments, under safe operation standards. However, the resulting dry bonded parts are safely handled, because their water extracts show pH lower than 9 down to neutrality, which is assigned to the rapid absorption of CO_2 from the atmosphere, transforming sodium hydroxide to carbonate. This is confirmed by the X-ray diffractogram of dry adhesive (Figure 1S).

The residual sodium carbonate does not by itself contribute to the adhesive properties. This is demonstrated by observing the preservation of the joints and of their mechanical properties measured following their immersion in NaCl aqueous solutions, where sodium carbonate is soluble.

X-ray microtomography provided additional information on the microstructure of the paper adhesive joints. Reconstructed

DOI: 10.1021/acsami.5b05310
ACS Appl. Mater. Interfaces 2015, 7, 18750−18758

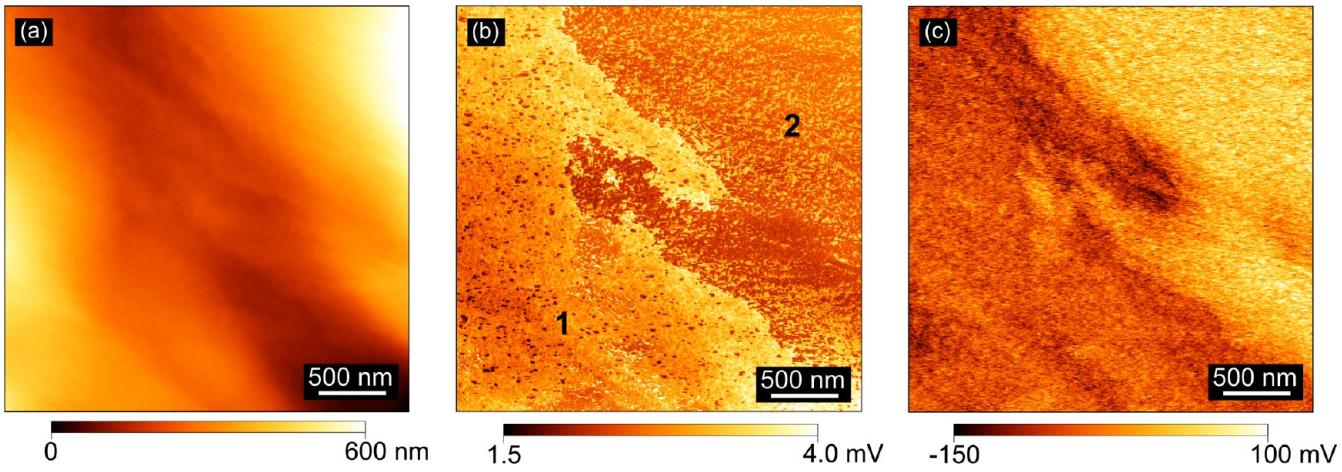

Figure 7. Images from cellulose adhesive dried on filter paper: (a) topography; (b) dC/dz: 1, bare fiber surface; 2, adhesive-coated fiber; and (c) electric potential.

X-ray images are shown for the as-received FP, for a single lap joint prepared with wet strips and for impregnated strip. The images report the attenuation of the X-rays when passing through the virtual sample slices cut from 3D reconstruction, using a false-color code that is also given beneath the images. Attenuation increases with the thickness of material in each voxel and with the electron density that increases with the average atom number in the voxel contents. Comparing our joints to the as-received FP, we see an increase in the X-ray attenuation, visually evidenced by the increase in the blue-colored image areas, together with the decrease of maroon and yellow areas. This confirms the SEM results: the adhesive solution fills the pores or voids between paper fibers, which produce only very low X-ray attenuation.

The decreased void volume is understood considering the shrinking effect of capillary adhesion during evaporation of water from the drying joints, together with pore filling by adhesive solids, in the dry joints. When the adhesive dries in a single lap joint, the residual solids can be estimated by using the amorphous cellulose density[28] (we adopted 1.385 g/cm^3, but other values are found in the literature[29,30]) and sodium carbonate density (2.540 g/cm^3).[31] Because we used 40 mg of adhesive to make each joint, the volume of residual solids is approximately 0.025 cm^3, divided between 0.014 cm^3 of amorphous cellulose and 0.011 cm^3 of sodium carbonate. Considering the two paper strips, the total paper volume in the adhesive joint is 0.06 cm^3 (2 × 1.00 cm × 2.50 cm × 0.012 cm). The as-received paper porosity calculated using microtomography data is 58%, so the total pore volume in the bonded area prior to joint formation is 0.035 cm^3. This estimate shows that the small amount of adhesive used is sufficient to fill ca. 70% of the filter paper pores. Figure 5c shows that most pores of the impregnated paper are coated, lowering paper porosity to 35%.

Pore filling by the adhesive produces a matrix interspersed with the paper fibers, creating the pattern often used in reinforced fiber materials. Moreover, the cellulose from adhesive should interact with the paper fibers by the various mechanisms that have been disclosed in the study of fiber-to-fiber bonding and will be discussed ahead.[32]

Previous studies on pressure-sensitive adhesives used AFM to reveal adhesive and adherend domains by phase-contrast.[33] We resorted to this technique to examine adjacent areas of filter paper, containing adhesive or not. The concurrent acquisition of AFM topography and phase-contrast did not provide useful information, as shown by comparing adjacent regions of plain filter paper and of paper partly coated with adhesive (Figure 6). In both cases, phase change due to edges dominates contrast. Figure 6 contains also electric potential and dC/dz maps, of the same area of partly coated filter paper, showing clearly contrasting domains.

Images acquired from a smaller area are given in Figure 7, where the adhesive covers most of the upper right quadrant. The AFM topography varies as expected for filter paper, up to 600 nm and no clear difference between the paper fibers and the area containing the adhesive film is observable. The dC/dz image allows identification of the adhesive domains due to the high contrast between the darker (containing adhesive) and brighter domains stemming from the change in the local sample capacitance.

The electric potential varies within −150 and 100 mV. We observe that the surface of the adhesive is positive and it is also easily identified. The darker rim of the brighter edge shows that negative charges accumulate outside the border of the positive adhesive film, forming a double-layer structure.

The positive electric potential areas correlate with the areas of low dC/dz signal, but contrast is sharper in the dC/dz map. We can use the dC/dz information to estimate the difference in the capacitance and therefore the difference in dielectric constant of the different sample areas. Using the marked positions in Figure 7b, the measured output signal proportional to dC/dz was 3.25 mV on filter paper and 2.15 mV on adhesive-coated filter paper, respectively. Assuming that the tip-air capacitance does not change over the sample, we can calculate the ratio between the two signals using the previously pointed out summation of the reciprocal capacitances and the extracted dC/dz values that are proportional to the local capacitance, obtaining the ratio

$$C_{ad} = 2C_{fp}$$

where C_{fp} and C_{ad} correspond to filter paper and adhesive, respectively. Because of the additive coupling, our estimate depends on C_{air}, which introduces an unknown variable into the calculations preventing the obtation of absolute values for the capacitances. Nevertheless, we clearly see that C_{ad} is twice the value of the combined effective capacitance over the filter paper region. As the dielectric constant of air is roughly equal to 1, we

DOI: 10.1021/acsami.5b05310
ACS Appl. Mater. Interfaces 2015, 7, 18750−18758

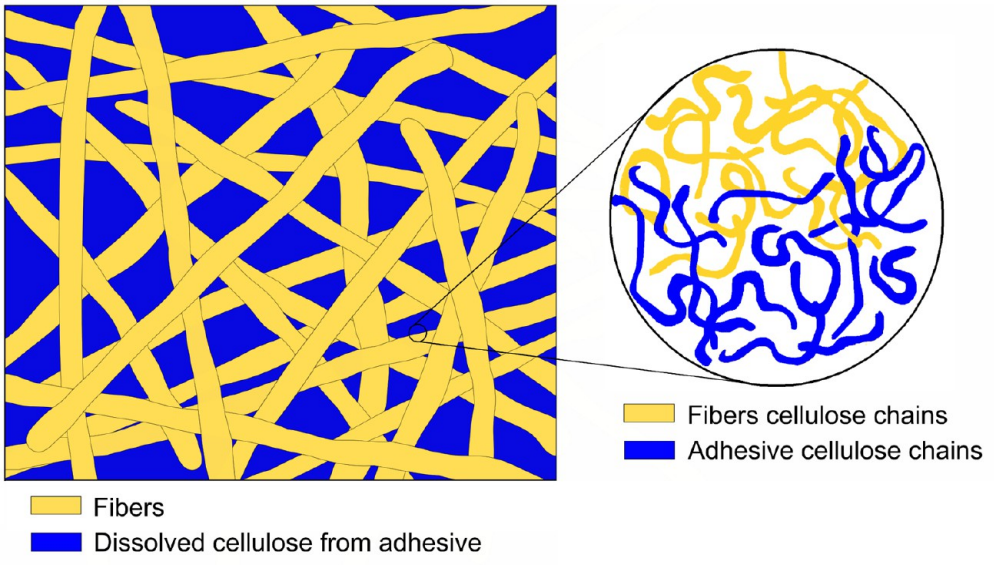

Figure 8. Graphic representation of a paper filter impregnated by the cellulose adhesive. The drawing to the left represents the upper layer from an actual SEM micrograph.

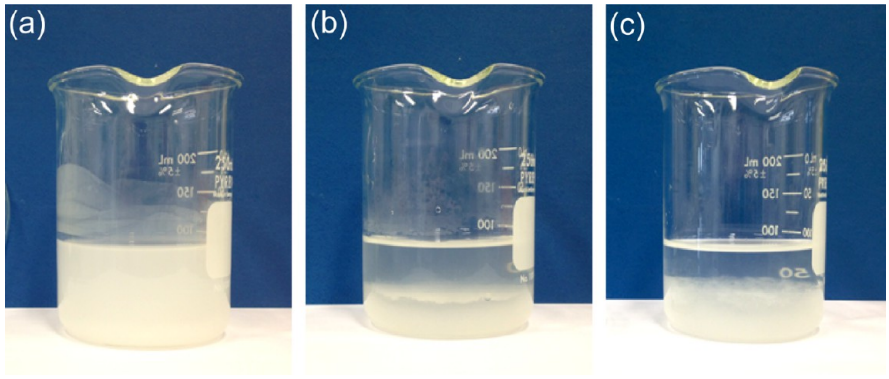

Figure 9. Pictures of aqueous dispersions of filter paper strips bonded with (a) PVA latex adhesive, (b) cellulose adhesive, and (c) sample without adhesive. Dispersions settled for 30 min.

can estimate the effective dielectric constant of the system over the filter paper as $\epsilon_{eff} = \epsilon_{fd}\ (z + H)/(z + \epsilon_{fd}{}^{*}H)$, where z is the tip−sample distance and H is the thickness of the filter paper with a dielectric constant ϵ_{fd}. As the thickness of the adhesive is much smaller than of the filter paper (its border is not observed in the topography image), we conclude that its dielectric constant is much higher than that of paper fibers, thus explaining the higher capacitance.

The higher dielectric constant of the adhesive compared to the underlying filter paper is assigned to higher water and ion content and gives rise to the observed charge accumulation on the domains with higher dielectric constant, imparting positive charge to them.[34]

Understanding the effective adhesion of paper sheets by cellulose solutions requires consideration of the intervening forces at the molecular level. Following the literature, cellulose chain−chain association is driven by Coulomb forces,[34,35] van der Waals interactions, hydrogen bonds, and following Lindman, hydrophobic interactions also play an important role.[36−38]

Otherwise, cellulose adhesion using cellulose solutions may be understood as just another successful case of bonding polymer materials with a solution of the same polymer, which in general promotes good adhesion[14] because of chain entanglements and surface plastic deformation. Cellulosic fiber bonding phenomena (fiber-to-fiber bond) have been recently investigated by Hirn and collaborators.[32,39] Generally, the adhesion between fibers occurs during drying, since the capillary force brings the surfaces into contact. Contact area would be limited by the fibers roughness, but the contact area between two fibers increases when they are wet and thus softer. Because the wet cellulosic surfaces have a hydrogel structure, the surface molecules have enough mobility to rearrange and to interdiffuse facilitating plastic deformation of the fibers surface.[39]

The cellulose solution makes an additional contribution to the fiber-to-fiber bond interactions, since it wets and softens the fibers with a medium that fills surface depressions with mobile cellulose chains, as illustrated in Figure 8.

Different from aqueous cellulose solution, liquefied wood (LW) used to bond wood substrates displays high adherend failure at low shear strength and poor water resistance.[40,41] For wet adhesion, the oxidation of cellulose surface is the current approach and this methodology can also resist mechanical efforts, obtaining average delamination force of ca. 17 N/m for polyvinylamine (PVAm) grafted onto carboxylated poly(*N*-isopropylacrylamide) microgels[24] and 25 N/m for PVAm with grafted TEMPO.[20] In this work, we also used peel tests to

DOI: 10.1021/acsami.5b05310
ACS Appl. Mater. Interfaces 2015, 7, 18750−18758

evaluate our adhesive joints but these always led to delamination of the paper sheets, themselves.

Finally, experiments were run to verify the behavior of paper bonded or impregnated with cellulose adhesive, when it is mechanically redispersed to produce cellulose pulp. A typical experimental result is shown in Figure 9. Redispersed paper glued with PVA adhesive forms a rather stable dispersion but water-dispersed plain paper dispersion settles within 30 min, the same as redispersed paper bonded with cellulose adhesive. Besides, the latter repulped dispersion did not show any extraneous materials, either floating or settling, as expected considering that it contains only cellulose and a small amount of sodium carbonate.

5. CONCLUSIONS

Cellulose alkaline aqueous solution is an adhesive for wet and dry cellulosic substrates. Single lap and butt joints made with paper sheets are mechanically more resistant than the cellulosic substrates themselves.

Cellulose-bonded paper joints are resistant to aqueous solutions and they form pulp by mechanical redispersion, undistinguishable from the as-received paper sheets. Thus, this adhesive is suitable for wet and dry paper, especially considering requirements for paper recycling.

Microscopy and microtomography results show a good penetration and filling of paper voids by the cellulose solution that dries forming an amorphous cellulose matrix. This makes a contribution additional to other known factors for adhesion of cellulosic materials, including electrostatic, van der Waals, hydrogen bonds, and hydrophobic interactions, together with chain interdiffusion.

■ ASSOCIATED CONTENT

Supporting Information

The Supporting Information is available free of charge on the ACS Publications website at DOI: 10.1021/acsami.5b05310.

Average results for uniaxial tensile tests and X-ray diffractogram of dried cellulose adhesive (PDF)

■ AUTHOR INFORMATION

Corresponding Author

*E-mail: fernagal@iqm.unicamp.br. Fax: +5519 3212 1004. Phone: +55 19 3518 3103.

Notes

The authors declare no competing financial interest.

■ ACKNOWLEDGMENTS

This work was supported by CNPq and Fapesp (Brazil) through Inomat, National Institute (INCT) for Complex Functional Materials and Fapesp-ETH, Bioenergy 2011. ESF is a graduate fellow from CNPq.

■ REFERENCES

(1) Klemm, D.; Philipp, B.; Heinze, T.; Heinze, U.; Wagenknecht, W. *Introduction* In *Comprehensive Cellulose Chemistry*; Wiley-VCH: Weinheim, Germany, 1998; pp 1−7.

(2) Olsson, C.; Westman, G. Direct Dissolution of Cellulose: Background, Means and Applications. In *Cellulose−Fundamental Aspects*; Van De Ven, T. G. M., Ed.; InTech: Rijeka, Croatia, 2013.

(3) Zhang, H.; Wu, J.; Zhang, J.; He, J. 1-Allyl-3-Methylimidazolium Chloride Room Temperature Ionic Liquid: A New and Powerful Nonderivatizing Solvent for Cellulose. *Macromolecules* **2005**, *38*, 8272−8277.

(4) Gannon, J. M.; Graveson, I.; Mortimer, S. A. Process for the Manufacture of Lyocell Fibre. U.S. 5 725 821 A, March 10, 1998.

(5) Kamide, K.; Okajima, K. Cleaving and Forming Hydrogen Bonds. U.S. 4 634 470 A, January 6, 1987.

(6) Isogai, A.; Atalla, R. H. Dissolution of cellulose in aqueous NaOH solutions. *Cellulose* **1998**, *5*, 309−319.

(7) Egal, M.; Budtova, T.; Navard, P. Structure of Aqueous Solutions of Microcrystalline Cellulose/Sodium Hydroxide below 0 °C and the Limit of Cellulose Dissolution. *Biomacromolecules* **2007**, *8*, 2282−2287.

(8) Yang, Q.; Fukuzumi, H.; Saito, T.; Isogai, A.; Zhang, L. Transparent Cellulose Films with High Gas Barrier Properties Fabricated from Aqueous Alkali/Urea Solutions. *Biomacromolecules* **2011**, *12*, 2766−2771.

(9) Cai, J.; Wang, L.; Zhang, L. Influence of Coagulation Temperature on Pore Size and Properties of Cellulose Membranes Prepared from NaOH−urea Aqueous Solution. *Cellulose* **2007**, *14*, 205−215.

(10) Qi, H.; Sui, X.; Yuan, J.; Wei, Y.; Zhang, L. Electrospinning of Cellulose-Based Fibers From NaOH/Urea Aqueous System. *Macromol. Mater. Eng.* **2010**, *295*, 695−700.

(11) Chen, X.; Burger, C.; Wan, F.; Zhang, J.; Rong, L.; Hsiao, B. S.; Chu, B.; Cai, J.; Zhang, L. Structure Study of Cellulose Fibers Wet-Spun from Environmentally Friendly NaOH/Urea Aqueous Solutions. *Biomacromolecules* **2007**, *8*, 1918−1926.

(12) Qi, H.; Cai, J.; Zhang, L.; Kuga, S. Properties of Films Composed of Cellulose Nanowhiskers and a Cellulose Matrix Regenerated from Alkali/Urea Solution. *Biomacromolecules* **2009**, *10*, 1597−1602.

(13) Adsul, M.; Soni, S. K.; Bhargava, S. K.; Bansal, V. Facile Approach for the Dispersion of Regenerated Cellulose in Aqueous System in the Form of Nanoparticles. *Biomacromolecules* **2012**, *13*, 2890−2895.

(14) Pizzi, A.; Mittal, K. L. *Handbook of Adhesive Technology, Revised and Expanded*; CRC Press: Boca Raton, FL, 2003.

(15) *Handbook of Paper and Paperboard Packaging Technology*, 2nd ed.; Kirwan, M. J., Ed.; Wiley: New York, 2013.

(16) Matlack, A. *Introduction to Green Chemistry*, second ed.; Taylor & Francis: New York, 2010.

(17) Vonfelden, R. S. Methods for Manufacturing Recyclable and Repulpable Packaging Materials. U.S. 2014 0 120 277 A1, May 1, 2014.

(18) Su, S.; Pelton, R. Bovine Serum Albumin (BSA) as an Adhesive for Wet Cellulose. *Cellulose* **2006**, *13*, 537−545.

(19) Li, X.; Pelton, R. Enhancing Wet Cellulose Adhesion with Proteins. *Ind. Eng. Chem. Res.* **2005**, *44*, 7398−7404.

(20) Pelton, R.; Ren, P.; Liu, J.; Mijolovic, D. Polyvinylamine- *graft* -TEMPO Adsorbs Onto, Oxidizes, and Covalently Bonds to Wet Cellulose. *Biomacromolecules* **2011**, *12*, 942−948.

(21) Notley, S. M.; Chen, W.; Pelton, R. Extraordinary Adhesion of Phenylboronic Acid Derivatives of Polyvinylamine to Wet Cellulose: A Colloidal Probe Microscopy Investigation. *Langmuir* **2009**, *25*, 6898−6904.

(22) Feng, X.; Pouw, K.; Leung, V.; Pelton, R. Adhesion of Colloidal Polyelectrolyte Complexes to Wet Cellulose. *Biomacromolecules* **2007**, *8*, 2161−2166.

(23) *Standard Test Method for Apparent Shear Strength of Single-Lap-Joint Adhesively Bonded Metal Specimens by Tension Loading (Metal-to-Metal)*; ASTM D1002-10 ; ASTM International: West Conshohocken, PA, 2010.

(24) Wen, Q.; Pelton, R. Microgel Adhesives for Wet Cellulose: Measurements and Modeling. *Langmuir* **2012**, *28*, 5450−5457.

(25) Magonov, S.; Alexander, J. Single-Pass Kelvin Force Microscopy and D *C* /d *Z* Measurements in the Intermittent Contact: Applications to Polymer Materials. *Beilstein J. Nanotechnol.* **2011**, *2*, 15−27.

(26) Sorokina, K. L.; Tolstikhina, A. L. Atomic Force Microscopy Modified for Studying Electric Properties of Thin Films and Crystals. Review. *Crystallogr. Rep.* **2004**, *49*, 476−499.

DOI: 10.1021/acsami.5b05310
ACS Appl. Mater. Interfaces 2015, 7, 18750−18758

(27) Abraham, D. W. Lateral Dopant Profiling in Semiconductors by Force Microscopy Using Capacitive Detection. *J. Vac. Sci. Technol., B: Microelectron. Process. Phenom.* **1991**, *9*, 703.
(28) Chen, W.; Lickfield, G. C.; Yang, C. Q. Molecular Modeling of Cellulose in Amorphous State. Part I: Model Building and Plastic Deformation Study. *Polymer* **2004**, *45*, 1063−1071.
(29) Mazeau, K.; Heux, L. Molecular Dynamics Simulations of Bulk Native Crystalline and Amorphous Structures of Cellulose. *J. Phys. Chem. B* **2003**, *107*, 2394−2403.
(30) Kontturi, E.; Lankinen, A. Following the Kinetics of a Chemical Reaction in Ultrathin Supported Polymer Films by Reliable Mass Density Determination with X-ray Reflectivity. *J. Am. Chem. Soc.* **2010**, *132*, 3678−3679.
(31) Perry, D. L. *Handbook of Inorganic Compounds*, second ed.; CRC Press: Boca Raton, FL, 2011; pp 374.
(32) Persson, B. N. J.; Ganser, C.; Schmied, F.; Teichert, C.; Schennach, R.; Gilli, E.; Hirn, U. Adhesion of cellulose fibers in paper. *J. Phys.: Condens. Matter* **2013**, *25*, 045002.
(33) Lei, C. H.; Ouzineb, K.; Dupont, O.; Keddie, J. L. Probing particle structure in waterborne pressure-sensitive adhesives with atomic force microscopy. *J. Colloid Interface Sci.* **2007**, *307*, 56−63.
(34) Linares, E. M.; Jannuzzi, S. A.; Galembeck, F. *Langmuir* **2011**, *24*, 15199−15205.
(35) Valadares, L. F.; Linares, E. M.; Bragança, F. C.; Galembeck, F. Electrostatic Adhesion of Nanosized Particles: The Cohesive Role of Water. *J. Phys. Chem. C* **2008**, *112*, 8534−8544.
(36) Lindman, B.; Karlström, G.; Stigsson, L. On the Mechanism of Dissolution of Cellulose. *J. Mol. Liq.* **2010**, *156*, 76−81.
(37) Medronho, B.; Romano, A.; Miguel, M. G.; Stigsson, L.; Lindman, B. Rationalizing Cellulose (in)solubility: Reviewing Basic Physicochemical Aspects and Role of Hydrophobic Interactions. *Cellulose* **2012**, *19*, 581−587.
(38) Kihlman, M.; Medronho, B. F.; Romano, A. L.; Germgård, U.; Lindman, B. Cellulose Dissolution in an Alkali Based Solvent: Influence of Additives and Pretreatments. *J. Braz. Chem. Soc.* **2013**, *24*, 295−303.
(39) Hirn, U.; Schennach, R. Comprehensive analysis of individual pulp fiber bonds quantifies the mechanisms of fiber bonding in paper. *Sci. Rep.* **2015**, *5*, 10503.
(40) Ugovšek, A.; Sever Škapin, A.; Humar, M.; Sernek, M. Microscopic Analysis of the Wood Bond Line Using Liquefied Wood as Adhesive. *J. Adhes. Sci. Technol.* **2013**, *27*, 1247−1258.
(41) Ugovšek, A.; Sernek, M. Characterisation of the Curing of Liquefied Wood by Rheometry, DEA and DSC. *Wood Sci. Technol.* **2013**, *47*, 1099−1111.

DOI: 10.1021/acsami.5b05310
ACS Appl. Mater. Interfaces 2015, 7, 18750−18758